Journal of Clinical and Translational Hepatology **2026**
DOI: 10.14218/JCTH.2026.00174

Original Article

Jaundice Is Associated with Intraoperative Hypotension, Suppressed Immune–endothelial NF-κB/EDN1 Signaling, and Impaired Vascular Cell Function

Gen Li[1#], Ming Cheng[2#], Jian He[1], Dengfeng Huang[3], Yingying Zhou[4], Yaohui Gao[3], Yuming Sun[5*] and Zhizhen Li[6*]

[1]Department of Intensive Care Unit, Eastern Hepatobiliary Surgery Hospital, Shanghai, China; [2]Department of Interventional Radiology, Eastern Hepatobiliary Surgery Hospital, Shanghai, China; [3]Department of Pathology, Shanghai Tenth People's Hospital Affiliated to Tongji University, Shanghai, China; [4]Department of Pathology, Eastern Hepatobiliary Surgery Hospital, Shanghai, China; [5]Department of Anesthesiology, Eastern Hepatobiliary Surgery Hospital, Shanghai, China; [6]Department of Biliary Tract Surgery I, Eastern Hepatobiliary Surgery Hospital, Shanghai, China

Received: March 09, 2026 | **Revised:** June 28, 2026 | **Accepted:** September 28, 2026 | **Published online:** November 17, 2026

Abstract

Background and Aims: Intraoperative hypotension (IOH) is a common and serious complication associated with increased perioperative morbidity and mortality. Although obstructive jaundice is often accompanied by hemodynamic instability, its mechanistic contribution to IOH remains unclear. In this study, we aimed to determine whether jaundice affects IOH and elucidate the underlying mechanism. ***Methods:*** Clinical data from 139 patients who underwent pancreatoduodenectomy were retrospectively analyzed for predictors of IOH. Vascular tissues from jaundiced and non-jaundiced patients were subjected to single-cell RNA sequencing for cell-specific molecular exploration. Key findings were validated by immunohistochemistry in a stratified random sample from the study cohort. In a rat bile duct ligation model, aortic endothelin-1 (EDN1) expression and vascular function were assessed by Western blotting and *ex vivo* vascular reactivity assays. The mechanism was investigated in primary mouse aortic endothelial cells under TNF-α stimulation with or without NF-κB pathway inhibition. ***Results:*** Multivariable logistic regression identified jaundice as an independent predictor of IOH (odds ratio, 2.328; 95% confidence interval, 1.027–5.276; $P = 0.043$). Jaundiced tissues exhibited vascular cell remodeling, characterized by increased proportions of endothelial cells and macrophages and decreased proportions of fibroblasts and smooth muscle cells. *EDN1* expression was significantly downregulated in jaundiced patients, and total bilirubin levels were negatively correlated with EDN1 protein expression ($P < 0.001$). Single-cell RNA sequencing of immune cells suggested suppression of the NF-κB pathway in jaundiced patients. In the bile duct ligation model, *EDN1* expression in aortic tissue showed a time-dependent decrease. In TNF-α-stimulated primary mouse aortic endothelial cells, bilirubin or NF-κB inhibition with BAY 11-7082 suppressed EDN1 expression. ***Conclusions:*** Biliary obstruction causing jaundice may contribute to IOH through suppression of NF-κB signaling and reduced endothelial EDN1 expression. These findings support further investigation of the NF-κB/EDN1 signaling axis as a potential therapeutic target for jaundice-associated IOH.

Citation of this article: Li G, Cheng M, He J, Huang D, Zhou Y, Gao Y, *et al*. Jaundice Is Associated with Intraoperative Hypotension, Suppressed Immune–endothelial NF-κB/EDN1 Signaling, and Impaired Vascular Cell Function. J Clin Transl Hepatol 2026. doi: 10.14218/JCTH.2026.00174.

Introduction

Intraoperative hypotension (IOH), defined as a sustained drop in arterial blood pressure during surgery, remains a frequent and clinically significant complication in perioperative care. Large retrospective series report that up to 65% of noncardiac surgeries experience at least one episode of mean arterial pressure (MAP) < 65 mmHg, and incidences as high as 80–90% have been observed depending on the definition used.[1,2] IOH has been consistently linked with adverse outcomes, including myocardial injury, acute kidney injury, stroke, increased length of hospital stay, and mortality.[3,4] Current prevention and treatment strategies typically include maintaining of intraoperative blood pressure targets (e.g., MAP ≥ 65 mmHg), prompt use of vasopressors, fluid optimization, reduction of anesthetic-induced vasodilation, and meticulous hemodynamic monitoring.[5,6] Despite these measures, there remains significant heterogeneity in IOH definitions, variable adoption of preventive protocols across centers, and limited mechanistic guidance regarding individual patient susceptibility and personalized thresholds.[1,7]

At the molecular and cellular level, IOH is increasingly un-

Keywords: Jaundice; Pancreaticoduodenectomy; Hypotension; Bilirubin; Risk factors; Endothelin-1; NF-kappa B; Vasoconstriction; ScRNA-seq.

[#]Contributed equally to this work as co-first authors.

[*]**Correspondence to:** Yuming Sun, Department of Anesthesiology, Eastern Hepatobiliary Surgery Hospital, 225 Changhai Road, Yangpu District, Shanghai 200438, China. ORCID: https://orcid.org/0000-0001-9347-3234. Tel: +86-133-0183-6930, E-mail: 13301836930@163.com; Zhizhen Li, Department of Biliary Tract Surgery I, Eastern Hepatobiliary Surgery Hospital, 225 Changhai Road, Yangpu District, Shanghai 200438, China. ORCID: https://orcid.org/0000-0002-2826-7589. Tel: +86-186-3666-0145, E-mail: lizhizhenlee@163.com.

Copyright: © 2026 The Author(s). This article has been published under the terms of Creative Commons Attribution-Noncommercial 4.0 International License (CC BY-NC 4.0), which permits noncommercial unrestricted use, distribution, and reproduction in any medium, provided that the following statement is provided. "This article has been published in *Journal of Clinical and Translational Hepatology* at https://doi.org/10.14218/JCTH.2026.00174 and can also be viewed on the Journal's website at http://www.jcthnet.com".

derstood not merely as a hemodynamic phenomenon but as a pathophysiological process involving impaired organ perfusion, ischemia–reperfusion injury, endothelial dysfunction, inflammatory activation, and microvascular dysregulation. For example, anesthetic induction-associated vasodilation and myocardial suppression may precipitate a mismatch between oxygen delivery and consumption, initiating inflammatory cascades that extend vascular instability beyond the intraoperative period.[8] However, mechanistic studies delineating how systemic insults translate into end-organ vascular responses remain insufficient, especially in the context of patient-specific vulnerability.

Obstructive jaundice (OJ) is a common clinical manifestation in hepatobiliary surgery that can be caused by tumors, stones, or trauma. Hypotension in patients with OJ during surgery may present as vascular hyporeactivity to adrenergic agonists.[9] Emerging but limited experimental evidence links OJ, reflecting elevated serum bilirubin and cholestatic stress, to vascular hyporeactivity.[10] Although data are scarce, patients with hepatic dysfunction and hyperbilirubinemia may exhibit altered vascular reactivity, vasodilation, and autonomic dysfunction, which could increase susceptibility to perioperative hypotensive episodes. This potential association remains underexplored in the literature. It is biologically plausible that elevated bilirubin could influence vascular tone through modulation of inflammatory signaling, endothelial function, and vasoactive mediators.[11] However, few studies have systematically explored the molecular mechanisms underlying jaundice-associated susceptibility to IOH.

In this study, we addressed this gap through a multilevel investigation. Clinically, we analyzed 139 patients undergoing pancreatoduodenectomy to evaluate the independent association of jaundice and other risk factors with IOH. At the molecular level, we employed single-cell RNA sequencing (scRNA-seq) of vascular tissue from jaundiced and non-jaundiced patients to define cell-type composition, cell–cell interactions, and endothelial gene expression, including *EDN1*, with a focus on the NF-κB signaling pathway and its downstream transcriptional networks. We further evaluated our core findings in clinical tissue sections using immunohistochemistry (IHC) and in a bile duct ligation (BDL) rat model, providing evidence that bilirubin exposure suppresses NF-κB signaling in endothelial cells and reduces endothelial EDN1 expression. Our data also suggest a potential link to impaired matrix metalloproteinase (MMP) regulatory responses in vascular smooth muscle and fibroblasts, although this relationship requires further investigation. These findings provide a mechanistic framework for jaundice-associated IOH and identify potential targets for further investigation aimed at improving perioperative vascular stability.

Methods

Clinical sample collection

Clinical data from 139 patients who underwent pancreatoduodenectomy at Eastern Hepatobiliary Surgery Hospital between June 2022 and March 2025 were retrospectively analyzed to identify factors associated with IOH. Collected variables included age, sex, body mass index (BMI), jaundice, history of heart disease, hypertension, diabetes, smoking, drinking, preoperative biliary drainage, intraoperative blood transfusion, intraoperative blood loss and jaundice grade. The study protocol was approved by the Ethics Committee of Eastern Hepatobiliary Surgery Hospital (Approval No. EHBH-KY2025-K104-P001). The requirement for informed consent was waived.

IOH was defined as a sustained drop in MAP below 65 mmHg for more than 10 min or a decrease of more than 20% from baseline MAP persisting for more than 10 min during the main intraoperative period from skin incision to wound closure, in accordance with the updated guidelines from the Association of Anesthetists and the British and Irish Hypertension Society.[12] Baseline MAP was calculated as the mean of three consecutive preoperative readings.

Single-cell RNA sequencing and data preprocessing

As an exploratory discovery phase to generate mechanistic hypotheses, we performed scRNA-seq on a limited number of fresh vascular specimens. Given the small sample size (n = 3), findings from this component were considered hypothesis-generating and were subsequently evaluated in independent clinical samples (IHC, n = 30) and *in vivo* animal models, as described below. Fresh gastroduodenal artery tissues isolated from surgical specimens were obtained from two patients with jaundice (mild and moderate/severe jaundice, respectively) and one patient with no obvious jaundice for scRNA-seq. Single-cell RNA libraries were constructed using the 10x Genomics Chromium GEM-X Single Cell 3′ Kit (v4) according to the manufacturer's protocol and sequenced on the Illumina NextSeq 2000 platform. Raw sequencing data were processed using Cell Ranger (v9.0.1) for filtering, alignment, quantification, and cell calling. Each sample contained more than 5,000 high-quality cells, with an average of more than 40,000 reads per cell, a median of more than 20,000 transcripts per cell, and more than 20,000 genes detected.

Single-cell RNA-seq data analysis

Data processing was performed in R (v3.6.3) using the Seurat package (v4).[13] Genes expressed in fewer than three cells were excluded, and low-quality cells (fewer than 200 detected genes or mitochondrial gene content > 10%) were filtered out. Normalization, identification of highly variable genes, scaling, and principal component analysis were performed using standard Seurat functions. Batch effects were corrected using Harmony.[14] Unsupervised clustering was performed at a resolution of 0.5, and cell clusters were visualized using uniform manifold approximation and projection. Cell types were annotated by cross-referencing cluster-specific differentially expressed genes (Wilcoxon rank-sum test) with canonical cell markers from the published literature.[13] Cell–cell communication analysis was conducted using CellChat (v2) to evaluate ligand–receptor interactions among vascular cell types.[15]

Pathway analysis

Gene set enrichment analysis was used to compare gene expression profiles between cell clusters,[16] referencing the Gene Ontology and Kyoto Encyclopedia of Genes and Genomes databases.[17,18] Ligand–receptor interaction data were obtained from CellTalkDB,[19] transcription factor–target regulatory data were obtained from ENCODE,[20] and protein interaction and post-translational modification data were sourced from Pathway Commons.[21,22]

Immunohistochemistry

Based on total bilirubin levels, patients were divided into three groups: no obvious jaundice (total bilirubin ≤ 34.2 μmol/L), mild jaundice (34.2< total bilirubin ≤85.0 μmol/L), and moderate/severe jaundice (total bilirubin >85.0 μmol/L). Ten patients were randomly selected from each group, and paraffin-embedded sections of resected surgical specimens from patients who underwent pancreatoduodenectomy were

systematically examined microscopically to identify arterial cross-sections, which were then subjected to hematoxylin and eosin staining and IHC for PECAM1, EDN1, ESM1, and TGF-β1. IHC was performed using standard protocols.[23] Briefly, after deparaffinization, rehydration, and microwave-based antigen retrieval, sections were blocked with normal goat serum and incubated overnight at 4°C with primary antibodies against CD31 (#16-0311, 1:200, Invitrogen), EDN1 (#MA3-005, 1:150, Invitrogen), ESM1 (#BS-3615R, 1:150, Invitrogen), or TGF-β1 (#141405, 1:80, BioLegend). After washing, sections were incubated with horseradish peroxidase (HRP)-conjugated secondary antibodies, developed with 3,3′-diaminobenzidine substrate, and counterstained with hematoxylin.

In vivo experiments

All animal procedures followed the Guide for the Care and Use of Laboratory Animals and were approved by the Animal Ethics Committee (No. SEU-IACUC-20260220123). Adult male Sprague–Dawley rats (200–280 g) were randomly assigned to sham or BDL groups (n = 6 each). BDL was performed as previously described.[24] Briefly, adult male Sprague–Dawley rats were anesthetized with pentobarbital sodium (50 mg/kg, i.p.). In the BDL group, the common bile duct was doubly ligated and transected between ligatures; sham-operated rats underwent the same procedure without ligation. Postoperative care included subcutaneous fluid and antibiotic prophylaxis. On postoperative day 7, blood samples were collected to measure total bilirubin, direct bilirubin, and alkaline phosphatase. A total bilirubin level > 50 μmol/L (5–10 × higher than in sham controls) indicated successful jaundice induction.

Ex vivo vascular reactivity

Ex vivo vascular reactivity was assessed using standard organ bath techniques as previously described.[25] On postoperative day 7, thoracic aortic rings (2–3 mm) from sham and BDL rats (n = 5 each) were mounted in an organ bath system (DMT, Denmark) containing oxygenated Krebs-Henseleit solution at 37°C. After a 90 min equilibration at 2.0 g resting tension, vessel viability was confirmed by KCl (60 mM) stimulation. Cumulative concentration–response curves to norepinephrine (NE, 10^{-9} to 3×10^{-6} M) and acetylcholine (ACh, 10^{-9} to 3×10^{-6} M) were generated. Isometric tension was recorded using a PowerLab data acquisition system (AD Instruments). Contractile responses to NE are expressed as absolute tension (g); relaxation responses to ACh are expressed as a percentage of NE-induced preconstriction.

Western blot analysis of rat vascular tissues

To investigate temporal changes in EDN1 expression, an additional cohort of rats (n = 4 per time point) underwent BDL surgery. At baseline (day 0, pre-operation) and on postoperative days 1, 3, 5, and 7, abdominal aortic tissues were collected and snap-frozen in liquid nitrogen. Western blot analysis was performed using standard protocols.[26] Proteins were extracted with radioimmunoprecipitation assay buffer containing protease and phosphatase inhibitors, quantified by bicinchoninic acid assay, separated by 12% sodium dodecyl sulfate–polyacrylamide gel electrophoresis, and transferred to polyvinylidene difluoride membranes. Membranes were blocked with 5% nonfat milk in Tris-buffered saline with Tween 20 and incubated overnight at 4°C with primary antibodies against EDN1 (#MA3-005, 1:200, Invitrogen) or β-actin (#4970, 1:2,000, Cell Signaling Technology). After incubation with HRP-conjugated secondary antibodies, protein bands were visualized using enhanced chemiluminescence and quantified using ImageJ software.

Cell culture and in vitro interventions

Primary mouse aortic endothelial cells (MAECs) were isolated from 6-week-old male C57BL/6 mice as previously described and cultured in endothelial cell medium under standard conditions.[27] Cells at passages 3–5 were used. After reaching 70% confluence and serum starvation (1% fetal bovine serum, 12 h), cells were treated with the indicated agents as described in prior studies.[28] The treatment conditions were: (1) vehicle control (0.1% dimethyl sulfoxide + 0.1% NaOH, 24 h); (2) TNF-α (20 ng/mL, 24 h); (3) bilirubin (20 μM, 2 h preincubation) followed by TNF-α cotreatment (24 h); and (4) BAY 11-7082 (5 μM, 1 h preincubation) followed by TNF-α cotreatment (24 h). After treatment, cells were harvested for Western blot analysis.

Western blot analysis of cultured cells

Total protein was extracted from treated MAECs using radioimmunoprecipitation assay lysis buffer. Western blot analysis was performed as described above. Primary antibodies included EDN1 (#MA3-005, 1:200, Invitrogen), phospho-p65 (#MA5-15160, 1:200, Invitrogen), p65 (#51-0500, 1:200, Invitrogen), phospho-IκBα (#MA5-15224, 1:200, Invitrogen), IκBα (#MA5-15132, 1:200, Invitrogen), MMP9 (#ab76003, 1:500, Abcam), MMP2 (#ab37150, 1:500, Abcam), β-actin (#4970, 1:2,000, Cell Signaling Technology), and β-tubulin (#MA5-16308, 1:1,000, Invitrogen).

Statistical analysis

Categorical and continuous clinical variables were compared between groups using the chi-square test and Mann–Whitney U test, respectively. Variables with $P < 0.1$ in univariate analyses were entered into a multivariable logistic regression model. Intraoperative blood transfusion was also included in the model as a prespecified clinically relevant confounder to identify independent predictors of IOH. The Mann–Whitney U test was also used for intergroup comparisons of gene expression levels, and Spearman's correlation was used to assess associations between total bilirubin and EDN1 protein expression. Two-tailed P values < 0.05 were considered statistically significant.

Results

Jaundice serves as an independent clinical predictor of IOH

Among 139 surgical patients (50 with IOH and 89 without IOH), comparison of clinical characteristics revealed differences in jaundice (P = 0.050) and age (P = 0.047) between the two groups (Table 1). Multivariable logistic regression identified jaundice (odds ratio, 2.328; 95% confidence interval, 1.027–5.276; P = 0.043) as an independent predictor of IOH (Table 2), supporting an independent association between jaundice and increased odds of IOH.

Jaundice is associated with remodeling of vascular cellular composition in patients

To investigate the molecular mechanisms underlying jaundice-associated hypotension, vascular tissues from two patients with jaundice and one patient without jaundice were analyzed by scRNA-seq. Seven major vascular cell types were identified in both groups: macrophages, fibroblasts, smooth muscle cells, monocytes, T cells, endothelial cells,

Table 1. Patient baseline clinical variables and univariate analysis

Clinical variables	Intraoperative hypotension (*n* = 50)	No intraoperative hypotension (*n* = 89)	*P* value
Median age (range), y	60.5 (42–78)	65 (36–80)	0.047
Sex, n (%)			0.283
Male	37 (74.00)	58 (65.17)	
Female	13 (26.00)	31 (34.83)	
Median BMI (range), kg/m^2	22.5 (16.5–30.8)	22.5 (15.6–32.1)	0.890
Jaundice, n (%)			0.050
Yes	39 (78.00)	55 (61.80)	
No	11 (22.00)	34 (38.20)	
History of heart disease, n (%)			0.822
Yes	5 (10.00)	10 (11.24)	
No	45 (90.00)	79 (88.76)	
Hypertension, n (%)			0.890
Yes	18 (36.00)	31 (34.83)	
No	32 (64.00)	58 (65.17)	
Diabetes, n (%)			0.308
Yes	17 (34.00)	23 (25.84)	
No	33 (66.00)	66 (74.16)	
Smoking, n (%)			0.246
Yes	19 (38.00)	24 (26.97)	
No	31 (62.00)	65 (73.03)	
Drinking, n (%)			0.565
Yes	11 (22.00)	16 (17.98)	
No	39 (78.00)	73 (82.02)	
Preoperative biliary drainage, n (%)			0.214
Yes	34 (68.00)	51 (57.30)	
No	16 (32.00)	38 (42.70)	
Operation duration (range), min	375 (215–675)	370 (176–670)	0.791
Intraoperative blood loss (range), mL	400 (100–1,900)	300 (100–1,000)	0.757
Intraoperative blood transfusion, n (%)			0.797
Yes	18 (36.00)	34 (38.20)	
No	32 (64.00)	55 (61.80)	
Total bilirubin on surgery day, μmol/L	65.65 (7.6–264.4)	46.30 (10.2–271.9)	0.159
Degree of jaundice on surgery day			0.169
No obvious jaundice	12 (24.00)	29 (32.58)	
Mild jaundice	20 (40.00)	37 (41.57)	
Moderate/severe jaundice	18 (36.00)	23 (25.84)	

Jaundice was defined as total bilirubin > 34.2 μmol/L at admission. The degree of jaundice was graded as follows: no obvious jaundice, total bilirubin ≤ 34.2 μmol/L; mild jaundice, total bilirubin > 34.2 to ≤ 85.0 μmol/L; moderate/severe jaundice, total bilirubin > 85.0 μmol/L. BMI, body mass index.

Table 2. Multivariable logistic regression analysis

Clinical variable	Coefficient (β)	SE	Wald χ^2	*P* value	OR	95% CI for OR
Age	−0.036	0.020	3.162	0.075	0.965	0.927–1.004
Jaundice	0.845	0.417	4.096	0.043	2.328	1.027–5.276
Intraoperative blood transfusion	−0.287	0.386	0.552	0.457	0.751	0.352–1.599

Jaundice was defined as total bilirubin > 34.2 μmol/L at admission. β, regression coefficient; CI, confidence interval; OR, odds ratio; SE, standard error.

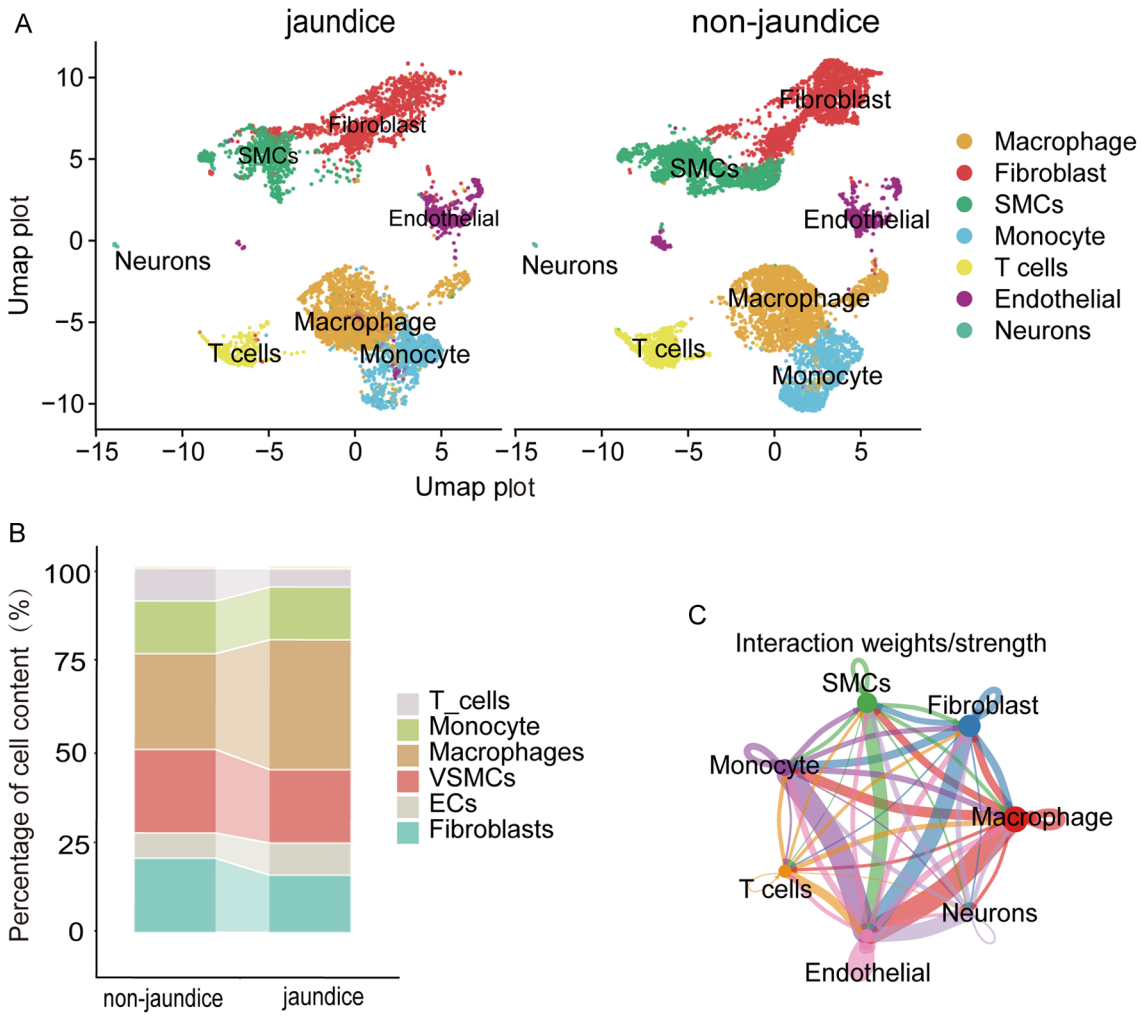


Fig. 1. Vascular cellular composition in patients with and without jaundice. A. Principal component analysis plot obtained from single-cell analysis, together with a comparison between the jaundice and non-jaundice groups. B. Stacked River plot of cell types in jaundice and non-jaundice samples in the scRNA-seq dataset. C. Cell–cell communication interactions among vascular cell types. scRNA-seq, single-cell RNA sequencing.

and neurons (Fig. 1A and Supplementary Fig. 1). Compared with non-jaundiced tissues, jaundiced samples exhibited an increased proportion of macrophages and endothelial cells and a decreased proportion of T cells, smooth muscle cells, and fibroblasts (Fig. 1B). Cell–cell communication analysis revealed that endothelial cells displayed the strongest interactions with macrophages, monocytes, fibroblasts, and smooth muscle cells (Fig. 1C and Supplementary Fig. 2), suggesting a central regulatory role for endothelial cells in vascular homeostasis.

Endothelial EDN1 expression is downregulated in jaundiced patients and correlates with bilirubin levels

Vascular endothelial cells were clustered into three subpopulations (clusters 0–2). Cluster 2 accounted for 20.6% of endothelial cells in non-jaundiced tissues but only 1.0% in jaundiced tissues (Fig. 2A). Cluster 2 showed high ESM1 expression, which served as a marker for this cluster (Fig. 2B). Nine genes, including *EDN1*, were significantly downregulated in endothelial cells from jaundiced samples (Fig. 2C). *EDN1* was predominantly expressed in the ESM1^{high} (cluster 2) endothelial cells (Fig. 2D). Given that *EDN1* encodes endothelin-1, a secreted vasoactive peptide that maintains vascular tone and blood pressure, these findings suggest that loss of *EDN1* in endothelial cells may contribute to hypotension in jaundice. IHC confirmed that EDN1 and ESM1 protein levels were significantly lower in jaundiced vascular tissues than in non-jaundiced tissues (Fig. 2E). Moreover, total bilirubin levels were negatively correlated with EDN1 expression ($r = -0.631$, $P < 0.001$) (Fig. 2F).

Single-cell transcriptomic profiling suggests reduced NF-κB signaling activity in vascular macrophages from jaundiced tissues

Analysis of vascular macrophages and monocytes revealed three immune subclusters with similar proportions between groups (Fig. 3A and B). Functional annotation using known biomarkers identified cluster 0 as tissue-resident macrophages (high *SELENOP* and *LYVE1*), cluster 1 as infiltrating monocytes (high *FCN1*, *S100A8*, and *S100A9*), and cluster 2 as proliferative macrophages (high *MKI67*, *TOP2A*, and *NUF2*) (Fig. 3C). Macrophage polarization analysis using the AddModuleScore function (Seurat v4.0) based on

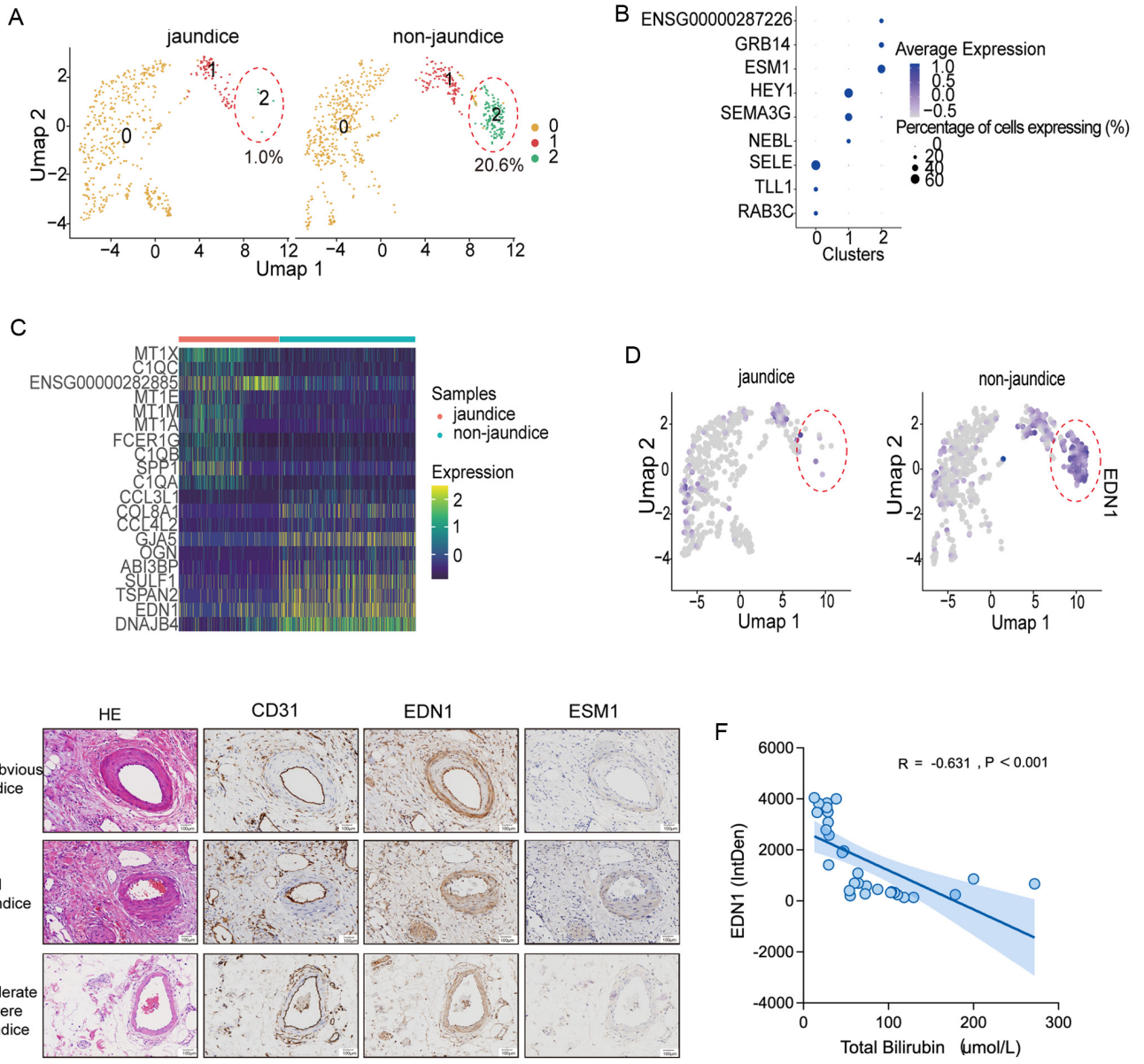


Fig. 2. Subpopulations and EDN1 expression features of endothelial cells in jaundiced vascular tissues. A. Principal component analysis plot of endothelial cells and comparison between the jaundice and non-jaundice groups. B. Marker genes and their expression levels in three endothelial cell subpopulations. C. Heatmap of differentially expressed genes between endothelial cells from jaundiced and non-jaundiced vascular tissues. D. EDN1 expression levels in endothelial cells from jaundiced and non-jaundiced samples. E. Immunohistochemical staining of CD31, EDN1, and ESM1 in vascular tissue from patients with varying bilirubin levels. F. Correlation between total serum bilirubin level and EDN1 expression in the vascular wall. CD31, cluster of differentiation 31; EDN1, endothelin-1; ESM1, endothelial cell-specific molecule 1.

established M1 (*TNF*, *IL6*, *CD86*) and M2 (*CD163*, *MRC1*, *ARG1*) gene signatures showed lower M1 score enrichment in a subset of tissue-resident macrophages from jaundiced tissues, suggesting a suppressed inflammatory state (Fig. 3D). Kyoto Encyclopedia of Genes and Genomes enrichment analysis revealed that genes downregulated in immune cells from the jaundiced group were significantly enriched in the NF-κB signaling pathway (Fig. 3E and Supplementary Fig. 3). Consistently, core NF-κB genes (*NFKBIA*, *NFKB1*, and *NFKB2*) and the cytokine-encoding gene *TGFB1* were among the downregulated genes in the jaundiced group (Fig. 3F). Subsequent immunohistochemical validation of TGF-β1 expression in the same clinical vascular tissue cohort is shown in Supplementary Figure 4.

Single-cell transcriptomic profiling reveals smooth muscle cell and fibroblast phenotypic switching with MMP2/9 downregulation in jaundiced vessels

Single-cell transcriptomic analysis of vascular fibroblasts and smooth muscle cells (SMCs) revealed distinct phenotypic shifts in jaundiced tissues (Fig. 4). Two fibroblast subpopulations were identified: homeostatic fibroblasts (high *CFD*, *ADH1B*, and *PI16*) and inflammation-associated fibroblasts (high *LYZ*, *HLA-DQA1*, and *C1QC*) (Fig. 4F). In jaundiced

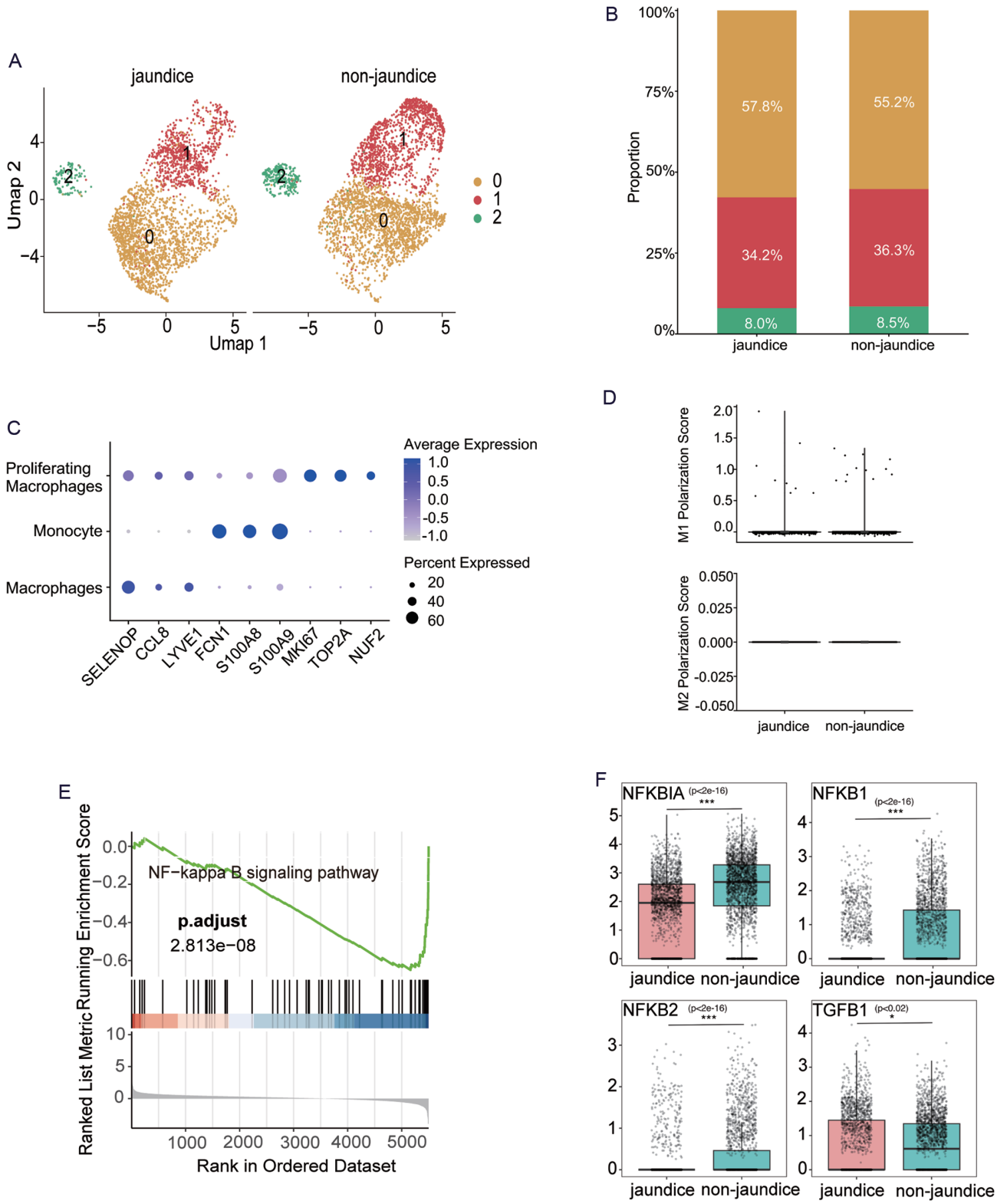


Fig. 3. Single-cell transcriptomic profiling of immune cells in vascular tissues from jaundiced and non-jaundiced patients. A. Principal component analysis plot of immune cells and comparison between the jaundice and non-jaundice groups. B. Cell proportions in the jaundiced and non-jaundiced groups. C. Dot plot of markers for immune cell subsets identified in the atlas. D. Box plots comparing M1 and M2 polarization scores of immune cells between jaundiced and non-jaundiced vascular tissues. E. Enrichment analysis of the NF-κB signaling pathway using downregulated genes in jaundiced immune cells. F. Box plots comparing expression levels of selected genes in immune cells between jaundiced and non-jaundiced patients. NF-κB, nuclear factor kappa B.

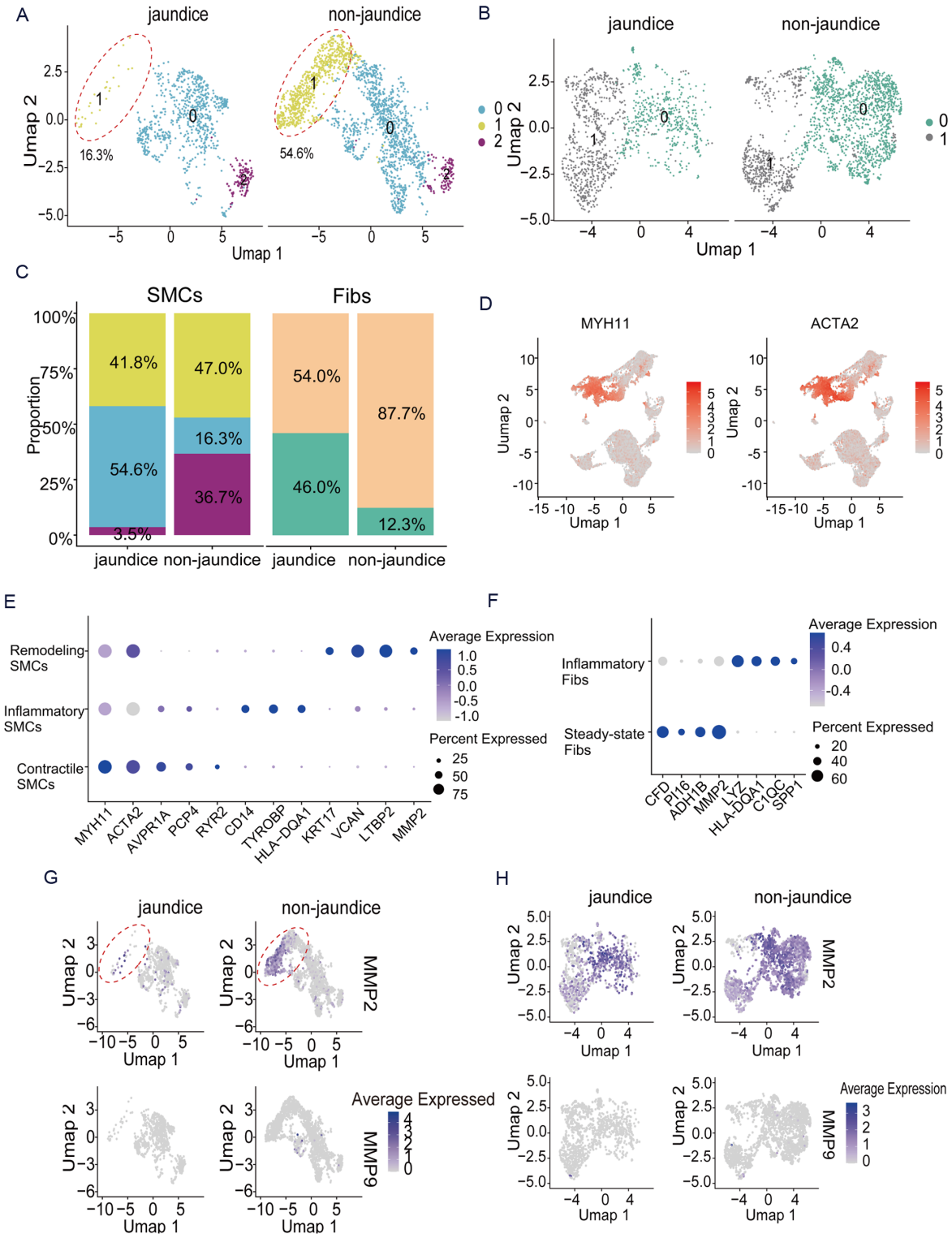


Fig. 4. Single-cell transcriptomic analysis of vascular smooth muscle cells and fibroblasts from jaundiced and non-jaundiced patients. A. Principal component analysis plot of vascular smooth muscle cells and comparison between the jaundice and non-jaundice groups. B. Principal component analysis plot of fibroblasts and comparison between the jaundice and non-jaundice groups. C. Stacked bar charts quantifying proportional changes in vascular smooth muscle cell and fibroblast subtypes between the two groups. D. UMAP plot of smooth muscle marker genes. E. Dot plot of markers for vascular smooth muscle cell subsets identified in the atlas. F. Dot plot of markers for fibroblast subsets identified in the atlas. G, H. UMAP plots of MMP2 and MMP9 expression in vascular smooth muscle cell and fibroblast subpopulations from non-jaundiced and jaundiced vascular tissues. MMP2, matrix metalloproteinase 2; MMP9, matrix metalloproteinase 9; UMAP, uniform manifold approximation and projection.

samples, the proportion of homeostatic fibroblasts markedly decreased from 87.7% to 54.0%, while inflammation-associated fibroblasts correspondingly increased from 12.3% to 46.0% (Fig. 4C), indicating a switch toward a proinflammatory stromal microenvironment. Similarly, three SMC subpopulations were distinguished: contractile SMCs (enriched for *AVPR1A* and *PCP4*), inflammatory SMCs (expressing *CD14* and *TYROBP*), and remodeling SMCs (marked by *KRT17*, *VCAN*, and *LTBP2*) (Fig. 4A and E). Lineage specificity was confirmed by the exclusive expression of *MYH11* and *ACTA2* in SMCs but not in fibroblasts (Fig. 4D). Notably, the expression of both MMP2 and MMP9 was prominently downregulated in SMCs and fibroblasts from jaundiced tissues (Fig. 4G and H). This reduction in MMP2/9 expression was observed across multiple subpopulations, particularly in the remodeling and inflammatory subsets. In summary, single-cell transcriptomic profiling reveals that vascular SMCs and fibroblasts from jaundiced patients undergo a pronounced shift from a contractile/homeostatic to an inflammatory/remodeling phenotype. This phenotypic transition is accompanied by downregulation of MMP2 and MMP9, key enzymes involved in extracellular matrix remodeling and vascular tone regulation. These molecular changes in the vascular wall may represent downstream effects of the EDN1 suppression observed in the jaundiced endothelium.

Bilirubin-induced EDN1 suppression via NF-κB is associated with vascular hyporeactivity in OJ

To directly assess the functional consequences of the molecular alterations observed in human jaundiced vessels, we performed *ex vivo* vascular reactivity measurements using thoracic aortic rings isolated from sham-operated and BDL rats on postoperative day 7. Aortic rings from BDL rats showed a trend toward a reduced contractile response to high-potassium (60 mM) depolarization compared with sham controls (sham: 0.792 ± 0.345 g vs. BDL: 0.384 ± 0.223 g; $P = 0.0574$, Fig. 5A), and the contractile response to NE was also lower in BDL rings, although this difference did not reach statistical significance (Supplementary Fig. 5). In rings precontracted with NE, endothelium-dependent relaxation to ACh was significantly impaired in the BDL group, with maximum relaxation (Rmax) significantly lower in BDL rings (39.6% ± 15.6%) than in sham controls (94.0% ± 11.5%; $P < 0.001$, Fig. 5A). In contrast, the relaxation response to the endothelium-independent vasodilator sodium nitroprusside was comparable between the two groups (Supplementary Fig. 5), suggesting that the intrinsic sensitivity of vascular smooth muscle to nitric oxide (NO) was not detectably altered. To determine whether the reduced EDN1 expression observed in human tissues also occurred in this model, we measured EDN1 protein levels in aortic tissues on days 0, 1, 3, 5, and 7 after BDL ($n = 4$ per time point). EDN1 expression remained comparable to baseline on day 1 but decreased sharply by day 3 and became nearly undetectable by day 7 (Fig. 5B and C), confirming a time-dependent suppression of EDN1 in the vessel wall after bile duct ligation. To further investigate the mechanism by which bilirubin regulates EDN1, we treated MAECs with TNF-α in the presence or absence of bilirubin (20 μM) or the NF-κB inhibitor BAY 11-7082. TNF-α stimulation increased the phosphorylation of IκBα and p65, as well as *EDN1* expression. Both bilirubin and BAY 11-7082 significantly reduced the phosphorylation levels of IκBα and p65 and suppressed TNF-α-induced upregulation of EDN1 (Fig. 5D and E). Additionally, expression of EDN1 and NF-κB pathway components in MAECs treated with bilirubin or BAY 11-7082 is shown in Supplementary Figure 6. In contrast, both MMP2 and MMP9 protein levels were moderately upregulated by TNF-α stimulation, and a moderate downregulation of MMP2 was observed in response to bilirubin treatment (Fig. 5F). Together, these data support a model in which bilirubin-induced NF-κB inhibition suppresses EDN1 expression in the vasculature and is associated with impaired endothelium-dependent relaxation and a trend toward reduced contractile responses in OJ.

Discussion

This study identifies jaundice as an independent clinical predictor of IOH and provides a convergent mechanistic framework integrating multilevel evidence from a clinical cohort, single-cell transcriptomics, histology, and animal models. Clinically, patients with jaundice had higher odds of IOH during pancreatoduodenectomy (odds ratio, 2.328; 95% confidence interval, 1.027–5.276; $P = 0.043$). Our single-cell transcriptomic analysis of vascular immune cells suggested reduction of NF-κB signaling in macrophages from jaundiced tissues, along with transcriptional downregulation of its downstream target, *TGFB1*. This observation, together with cell–cell communication analysis, suggests a possible link between the immune microenvironment and endothelial function in hyperbilirubinemia. However, subsequent immunohistochemical validation of TGF-β1 expression in the same clinical vascular tissue cohort showed no significant correlation with serum bilirubin levels ($r = 0.054$, $P = 0.777$). This negative finding should be interpreted with caution, as immunohistochemistry of formalin-fixed, paraffin-embedded tissue cannot distinguish between latent and bioactive TGF-β1, and cell-type-specific signals may be diluted in full-thickness vascular sections.[29–31] Therefore, while the transcriptional link between NF-κB suppression and *TGFB1* downregulation in immune cells was observed, our protein-level evidence does not support a direct mechanistic role for this axis in immune–endothelial crosstalk. Further investigation is warranted. Importantly, our data converge on a central finding supported by multiple lines of evidence: endothelial EDN1 expression is downregulated in jaundiced vascular tissues, inversely correlates with serum bilirubin levels, and is suppressed by bilirubin through inhibition of the NF-κB pathway in endothelial cells.[32,33] The resultant loss of EDN1 may impair fibroblast and smooth muscle MMP2/9 expression, thereby weakening vascular contractile reserve. Notably, while an EDN1–MMP2/9 association was suggested by the human transcriptomic data, our acute *in vitro* experiments in primary endothelial cells did not recapitulate this effect (Fig. 5F), suggesting that regulation of MMP2/9 by EDN1 in the vascular wall may require a chronic inflammatory microenvironment or involve paracrine signaling from other cell types (e.g., macrophages and fibroblasts) that are absent in monoculture. Future coculture or long-term exposure studies are warranted to elucidate the precise temporal and cellular requirements for EDN1-driven MMP regulation.

Previous clinical studies have described vascular hyporeactivity in patients with OJ,[9,34,35] yet the mechanistic basis remained unclear. Prior work attributed hypotension mainly to reduced vascular responsiveness to adrenergic agents or increased NO production.[36–38] Our findings extend these observations by providing cell-resolved transcriptomic evidence suggesting that bilirubin may modulate the immune–endothelial axis via NF-κB/EDN1 signaling. However, our *ex vivo* data also reveal a more complex picture: in the rat BDL model, aortic rings exhibited impaired endothelium-dependent relaxation (reduced Rmax to ACh) alongside apparently preserved smooth muscle sensitivity to NO (unchanged response to sodium nitroprusside). This dissociation be-

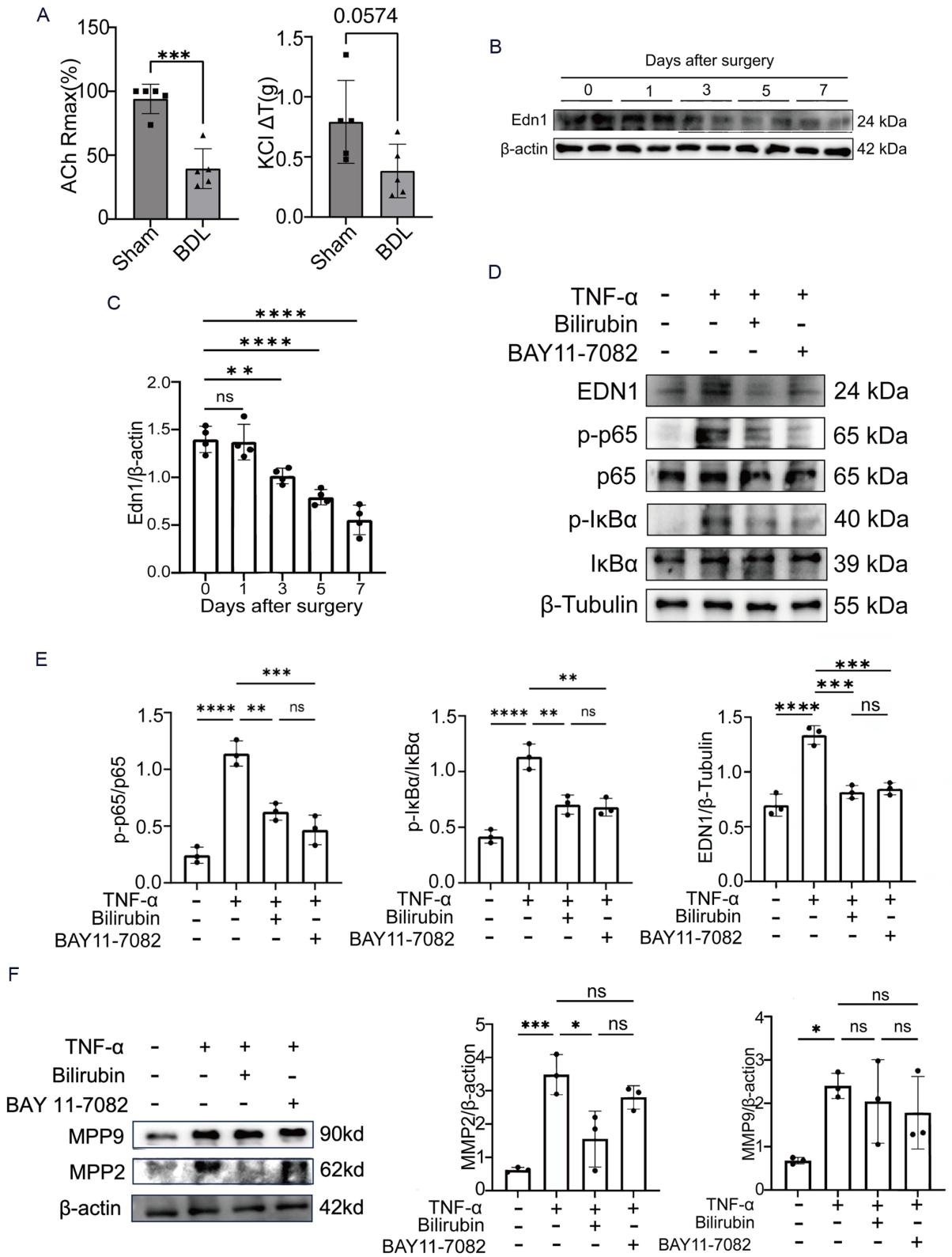


Fig. 5. Vascular reactivity and EDN1 expression in BDL rats and MAECs. A. ACh relaxation and KCl contraction in aortic rings. B, C. EDN1 expression in aortic tissues after BDL. D, E. EDN1, p-p65, and p-IκBα levels in treated MAECs. F. MMP2 and MMP9 levels in treated MAECs. ACh, acetylcholine; BDL, bile duct ligation; EDN1, endothelin-1; KCl, potassium chloride; MAEC, mouse aortic endothelial cell; MMP2, matrix metalloproteinase 2; MMP9, matrix metalloproteinase 9; p-IκBα, phosphorylated IκBα; p-p65, phosphorylated p65.

tween ACh and sodium nitroprusside responses suggests a broader state of generalized endothelial dysfunction in acute cholestasis, which may contribute to vascular hyporeactivity independently of the EDN1/MMP axis. Future studies should investigate whether this impaired endothelial function reflects direct bilirubin toxicity, altered shear stress, or additional circulating factors unique to the cholestatic milieu.

A critical question raised by our findings concerns the context-dependent roles of EDN1 in vascular tone. Classically, EDN1 binding to endothelin type A (ETA) receptors on vascular smooth muscle cells induces sustained vasoconstriction, whereas activation of endothelial endothelin type B (ETB) receptors triggers NO and prostacyclin release, leading to transient vasodilation.[39] Under physiologic conditions, the net pressor effect of EDN1 predominates.[40] In OJ, however, EDN1 downregulation is expected to disproportionately impair ETA-mediated vasoconstrictive reserve, as simultaneous suppression of NF-κB may also limit inducible nitric oxide synthase (iNOS)/NO pathway activity,[41] thereby reducing the counterbalancing vasodilatory component of EDN1 deficiency. The net effect may be a loss of vasoconstrictive capacity rather than active vasodilation, which could help explain higher intraoperative vasopressor requirements in jaundiced patients without baseline hypotension. Similarly, the role of NF-κB in blood pressure regulation is highly context-dependent. In sepsis, excessive NF-κB activation drives iNOS upregulation and overproduction of NO, leading to vasoplegic hypotension.[42–44] In contrast, our study suggests that, in chronic cholestatic jaundice, bilirubin-induced NF-κB suppression may contribute to diminished vasoconstrictive reserve. Although both conditions can be associated with hypotension, the underlying mechanisms may differ: sepsis-associated hypotension is often driven by excessive active vasodilation, whereas jaundice-associated hypotension may reflect reduced active vasoconstriction. Notably, although NF-κB suppression may also limit iNOS-mediated vasodilation, this effect may be insufficient to compensate for loss of EDN1-driven contractile reserve. This distinction highlights the context-dependent role of NF-κB in vascular homeostasis and may help explain why NF-κB suppression can predispose jaundiced patients to IOH.

Regarding the role of MMPs in the vascular dysfunction observed here, although MMPs are classically recognized for their role in extracellular matrix degradation, accumulating evidence demonstrates that MMP-2 and MMP-9 directly regulate vascular tone through nonmatrix mechanisms.[45] Specifically, MMPs can induce vasoconstriction by cleaving vasodilatory peptides into less active fragments, generating the potent vasoconstrictor endothelin 1-32 from big ET-1, transactivating the epidermal growth factor receptor, and enhancing vascular smooth muscle contractile responses. Consistent with our findings, MMP-2 and MMP-9 activities have been linked to increased arterial stiffness and systolic hypertension in clinical populations.[46] In the context of our study, however, the observed downregulation of MMP2/9 may represent a loss of vascular contractile reserve rather than an active vasodilatory mechanism.

These findings carry several translational implications for perioperative care. First, they provide a mechanistic rationale for preoperative risk stratification: serum bilirubin, as a readily available clinical parameter, remains a useful indicator, and future studies should explore whether tissue-level changes in EDN1 and MMP2/9 are reflected in circulating biomarkers to identify jaundiced patients at higher risk for IOH. Second, the NF-κB/EDN1 signaling axis identifies potential intervention nodes. One approach to investigate would be to reduce bilirubin burden preoperatively (e.g., via endoscopic biliary drainage).[47] When decompression is not feasible, strategies to restore vasoconstrictive reserve must be carefully calibrated. Given the dual effects of EDN1—predominantly ETA-mediated vasoconstriction and ETB-mediated vasodilation—a selective ETA receptor agonist may be more rational than nonselective EDN1 supplementation, although such agents remain largely investigational.[48] In future studies, direct vasoconstrictors such as vasopressin, whose signaling pathway is independent of the NF-κB/EDN1 signaling axis, could be evaluated as potential alternatives to bypass impaired vasoconstrictive mechanisms.[49] These interventions were not tested in this study. Third, these mechanistic insights reinforce the rationale for individualized, goal-directed hemodynamic management in jaundiced patients, with anticipation of elevated vasopressor requirements.

Several limitations of this study should be acknowledged. First, the generalizability of our clinical findings is limited by a cohort size (n = 139) suitable for exploratory but not definitive analysis, and validation in larger, multicenter cohorts is needed. Second, the scRNA-seq analysis was performed on a limited number of human vascular samples (n = 3), which constrains the statistical power for detecting rare cell populations and may not capture the full spectrum of inter-individual variability. Third, this study focused on major vascular tissues (the gastroduodenal artery in humans and the aorta in rats), which may not fully represent systemic vascular responses during anesthesia, particularly in resistance arterioles. Fourth, while our transcriptomic data suggest a link between EDN1 deficiency and MMP2/9 downregulation, the direct causal relationship has not been fully established in a reductionist *in vitro* system. Definitive confirmation will require future studies using coculture models of endothelial cells with vascular smooth muscle cells or fibroblasts to recapitulate the paracrine signaling environment of the vessel wall.

Conclusions

In conclusion, this study identifies jaundice as an independent predictor of IOH and provides a multilevel mechanistic framework linking hyperbilirubinemia to impaired vascular contractile reserve. Our findings suggest that bilirubin exposure suppresses NF-κB signaling in endothelial cells, and scRNA-seq data further suggest similar suppression in vascular immune cells; together, these changes may contribute to EDN1 downregulation. Disruption of NF-κB/EDN1 signaling may impair endothelium-dependent relaxation and increase susceptibility to hemodynamic instability during surgery. These findings provide a mechanistic rationale for preoperative risk stratification and support further investigation of the NF-κB/EDN1 signaling axis as a potential therapeutic target for perioperative vascular management in OJ.

Supporting information

Supplementary material for this article is available at https://doi.org/10.14218/JCTH.2026.00174.

Acknowledgments

We thank the Eastern Hepatobiliary Surgery Hospital, Naval Medical University, for supporting this research.

Funding

This work was supported by the Research on key techniques of constructing individualized treatment model of intrahepat-

ic cholangiocarcinoma based on real world data and artificial intelligence technology, Shanghai Municipal Education Commission (Grant No. 2024RGYB005), Shanghai Anticancer Association EYAS PROJECT (Grant No. SACA-CY24C1).

Conflict of interest

The authors have no conflict of interests related to this publication.

Author contributions

GL, JH and ZL conceptualized the study and designed the research. GL and MC extracted and sequenced the single-cell transcriptome. YS, GL and DH prepared tissue samples and performed the cell experiments. GL and YZ performed the animal experiments. GL and DH contributed to data analysis and interpretation. GL, YG and ZL wrote and revised the article with the suggestions of other co-authors. All authors have approved the final version and publication of the manuscript.

Ethical statement

This study was approved by Ethics Committee of Eastern Hepatobiliary Surgery Hospital (Approval No. EHBH-KY2025-K104-P001). The study was conducted in accordance with the Declaration of Helsinki (as revised in 2024). All study data and surgical specimens have been fully deidentified, and confidential information of patients has been deleted in accordance with the CIOMS/WHO International Ethical Guidelines for Health-related Research Involving Humans (2016). Consequently, the need for informed consent for the use of clinical data and surgical specimens was waived by the Ethics Committee of Eastern Hepatobiliary Surgery Hospital. This waiver applied to all components of the study, including the retrospective clinical cohort, the fresh vascular specimens used for single-cell RNA sequencing, and the archived paraffin-embedded tissues used for immunohistochemistry, all of which were derived from the same surgical cohort at this institution. Animal procedures followed the Guide for the Care and Use of Laboratory Animals and were approved by the Animal Ethics Committee (SEU-IACUC-20260220123). All animals received humane care.

Data sharing statement

The datasets used or analyzed during the current study are available from the corresponding author on reasonable request.

References

[1] Wijnberge M, Schenk J, Bulle E, Vlaar AP, Maheshwari K, Hollmann MW, *et al*. Association of intraoperative hypotension with postoperative morbidity and mortality: systematic review and meta-analysis. BJS Open 2021;5(1):zraa018. doi:10.1093/bjsopen/zraa018, PMID:33609377.
[2] Bijker JB, van Klei WA, Kappen TH, van Wolfswinkel L, Moons KG, Kalkman CJ. Incidence of intraoperative hypotension as a function of the chosen definition: literature definitions applied to a retrospective cohort using automated data collection. Anesthesiology 2007;107(2):213–220. doi:10.1097/01.anes.0000270724.40897.8e, PMID:17667564.
[3] Sharma SK, McCauley J, Cottam D, Mattar SG, Holover S, Dallal R, *et al*. Acute changes in renal function after laparoscopic gastric surgery for morbid obesity. Surg Obes Relat Dis 2006;2(3):389–392. doi:10.1016/j.soard.2006.02.002, PMID:16925359.
[4] Salmasi V, Maheshwari K, Yang D, Mascha EJ, Singh A, Sessler DI, *et al*. Relationship between Intraoperative Hypotension, Defined by Either Reduction from Baseline or Absolute Thresholds, and Acute Kidney and Myocardial Injury after Noncardiac Surgery: A Retrospective Cohort Analysis. Anesthesiology 2017;126(1):47–65. doi:10.1097/ALN.0000000000001432, PMID:27792044.
[5] Davies SJ, Vistisen ST, Jian Z, Hatib F, Scheeren TWL. Ability of an Arterial Waveform Analysis-Derived Hypotension Prediction Index to Predict Future Hypotensive Events in Surgical Patients. Anesth Analg 2020;130(2):352–359. doi:10.1213/ANE.0000000000004121, PMID:30896602.
[6] Hatib F, Jian Z, Buddi S, Lee C, Settels J, Sibert K, *et al*. Machine-learning Algorithm to Predict Hypotension Based on High-fidelity Arterial Pressure Waveform Analysis. Anesthesiology 2018;129(4):663–674. doi:10.1097/ALN.0000000000002300, PMID:29894315.
[7] Lai CJ, Cheng YJ, Han YY, Hsiao PN, Lin PL, Chiu CT, *et al*. Hypotension prediction index for prevention of intraoperative hypotension in patients undergoing general anesthesia: a randomized controlled trial. Perioper Med (Lond) 2024;13(1):57. doi:10.1186/s13741-024-00414-7, PMID:38879506.
[8] Saugel B, Bebert EJ, Briesenick L, Hoppe P, Greiwe G, Yang D, *et al*. Mechanisms contributing to hypotension after anesthetic induction with sufentanil, propofol, and rocuronium: a prospective observational study. J Clin Monit Comput 2022;36(2):341–347. doi:10.1007/s10877-021-00653-9, PMID:33523352.
[9] Yang LQ, Song JC, Irwin MG, Song JG, Sun YM, Yu WF. A clinical prospective comparison of anesthetics sensitivity and hemodynamic effect among patients with or without obstructive jaundice. Acta Anaesthesiol Scand 2010;54(7):871–877. doi:10.1111/j.1399-6576.2010.02222.x, PMID:20236100.
[10] Chen M, Zhang Y, Wang H, Yang H, Yin W, Xu S, *et al*. Inhibition of the norepinephrine transporter rescues vascular hyporeactivity to catecholamine in obstructive jaundice. Eur J Pharmacol 2021;900:174055. doi:10.1016/j.ejphar.2021.174055, PMID:33775645.
[11] Maruhashi T, Kihara Y, Higashi Y. Bilirubin and Endothelial Function. J Atheroscler Thromb 2019;26(8):688–696. doi:10.5551/jat.RV17035, PMID:31270300.
[12] McCormack T, Wickham A, McDonagh STJ, Wiles MD, Faconti L, Brooks R, *et al*. Measurement and management of adult blood pressure in the peri-operative period: updated guidelines from the Association of Anaesthetists and the British and Irish Hypertension Society. Anaesthesia 2026;81(3):402–414. doi:10.1111/anae.70082, PMID:41532177.
[13] Hao Y, Hao S, Andersen-Nissen E, Mauck WM 3rd, Zheng S, Butler A, *et al*. Integrated analysis of multimodal single-cell data. Cell 2021;184(13):3573–3587.e29. doi:10.1016/j.cell.2021.04.048, PMID:34062119.
[14] Su M, Pan T, Chen QZ, Zhou WW, Gong Y, Xu G, *et al*. Data analysis guidelines for single-cell RNA-seq in biomedical studies and clinical applications. Mil Med Res 2022;9(1):68. doi:10.1186/s40779-022-00434-8, PMID:36461064.
[15] Jin S, Plikus MV, Nie Q. CellChat for systematic analysis of cell-cell communication from single-cell transcriptomics. Nat Protoc 2025;20(1):180–219. doi:10.1038/s41596-024-01045-4, PMID:39289562.
[16] Subramanian A, Tamayo P, Mootha VK, Mukherjee S, Ebert BL, Gillette MA, *et al*. Gene set enrichment analysis: a knowledge-based approach for interpreting genome-wide expression profiles. Proc Natl Acad Sci U S A 2005;102(43):15545–15550. doi:10.1073/pnas.0506580102, PMID:16199517.
[17] Harris MA, Clark J, Ireland A, Lomax J, Ashburner M, Foulger R, *et al*. The Gene Ontology (GO) database and informatics resource. Nucleic Acids Res 2004;32(Database issue):D258–D261. doi:10.1093/nar/gkh036, PMID:14681407.
[18] Kanehisa M, Goto S. KEGG: kyoto encyclopedia of genes and genomes. Nucleic Acids Res 2000;28(1):27–30. doi:10.1093/nar/28.1.27, PMID:10592173.
[19] Shao X, Liao J, Li C, Lu X, Cheng J, Fan X. CellTalkDB: a manually curated database of ligand-receptor interactions in humans and mice. Brief Bioinform 2021;22(4):bbaa269. doi:10.1093/bib/bbaa269, PMID:33147626.
[20] ENCODE Project Consortium. A user's guide to the encyclopedia of DNA elements (ENCODE). PLoS Biol 2011;9(4):e1001046. doi:10.1371/journal.pbio.1001046, PMID:21526222.
[21] Rodchenkov I, Babur O, Luna A, Aksoy BA, Wong JV, Fong D, *et al*. Pathway Commons 2019 Update: integration, analysis and exploration of pathway data. Nucleic Acids Res 2020;48(D1):D489–D497. doi:10.1093/nar/gkz946, PMID:31647099.
[22] Wong JV, Franz M, Siper MC, Fong D, Durupinar F, Dallago C, *et al*. Author-sourced capture of pathway knowledge in computable form using Biofactoid. Elife 2021;10:e68292. doi:10.7554/eLife.68292, PMID:34860157.
[23] Lin F, Chen Z. Standardization of diagnostic immunohistochemistry: literature review and geisinger experience. Arch Pathol Lab Med 2014;138(12):1564–1577. doi:10.5858/arpa.2014-0074-RA, PMID:25427038.
[24] Mariotti V, Strazzabosco M, Fabris L, Calvisi DF. Animal models of biliary injury and altered bile acid metabolism. Biochim Biophys Acta Mol Basis Dis 2018;1864(4 Pt B):1254–1261. doi:10.1016/j.bbadis.2017.06.027, PMID:28709963.
[25] Tian Z, Ning H, Wang X, Wang Y, Han T, Sun C. Endothelial Autophagy Promotes Atheroprotective Communication Between Endothelial and Smooth Muscle Cells via Exosome-Mediated Delivery of miR-204-5p. Arterioscler Thromb Vasc Biol 2024;44(8):1813–1832. doi:10.1161/ATVBAHA.123.319993, PMID:38957984.
[26] Taylor SC, Rosselli-Murai LK, Crobeddu B, Plante I. A critical path to producing high quality, reproducible data from quantitative western blot experiments. Sci Rep 2022;12(1):17599. doi:10.1038/s41598-022-22294-x, PMID:36266411.
[27] Lu L, Jang S, Zhu J, Qin Q, Sun L, Sun J. Nur77 mitigates endothelial dysfunction through activation of both nitric oxide production and antioxidant pathways. Redox Biol 2024;70:103056. doi:10.1016/j.redox.2024.103056, PMID:38290383.
[28] Liu L, Qiu L, Xue J, Zhong C, Qin M, Zhang Y, *et al*. Saponins from Allium macrostemon Bulbs Attenuate Endothelial Inflammation and Acute

Lung Injury via the NF-κB/VCAM-1 Pathway. Molecules 2024;29(6):1239. doi:10.3390/molecules29061239, PMID:38542876.
[29] Tie Y, Tang F, Peng D, Zhang Y, Shi H. TGF-beta signal transduction: biology, function and therapy for diseases. Mol Biomed 2022;3(1):45. doi:10.1186/s43556-022-00109-9, PMID:36534225.
[30] Tsutsumi Y. Pitfalls and Caveats in Applying Chromogenic Immunostaining to Histopathological Diagnosis. Cells 2021;10(6):1501. doi:10.3390/cells10061501, PMID:34203756.
[31] Shah M, Polónia A, Curado M, Vale J, Janowczyk A, Eloy C. Impact of Tissue Thickness on Computational Quantification of Features in Whole Slide Images for Diagnostic Pathology. Endocr Pathol 2025;36(1):10. doi:10.1007/s12022-025-09855-2, PMID:40198470.
[32] Quehenberger P, Bierhaus A, Fasching P, Muellner C, Klevesath M, Hong M, *et al*. Endothelin 1 transcription is controlled by nuclear factor-kappaB in AGE-stimulated cultured endothelial cells. Diabetes 2000;49(9):1561–1570. doi:10.2337/diabetes.49.9.1561, PMID:10969841.
[33] Zhang S, Li X, Liu S, Zhang W, Li M, Qiao C. Research progress on the role of ET-1 in diabetic kidney disease. J Cell Physiol 2023;238(6):1183–1192. doi:10.1002/jcp.31023, PMID:37063089.
[34] Green J, Better OS. Systemic hypotension and renal failure in obstructive jaundice-mechanistic and therapeutic aspects. J Am Soc Nephrol 1995;5(11):1853–1871. doi:10.1681/ASN.V5111853, PMID:7620083.
[35] Liu J, Qu J, Chen H, Ge P, Jiang Y, Xu C, *et al*. The pathogenesis of renal injury in obstructive jaundice: A review of underlying mechanisms, inducible agents and therapeutic strategies. Pharmacol Res 2021;163:105311. doi:10.1016/j.phrs.2020.105311, PMID:33246170.
[36] Vane JR, Anggård EE, Botting RM. Regulatory functions of the vascular endothelium. N Engl J Med 1990;323(1):27–36. doi:10.1056/NEJM199007053230106, PMID:2113184.
[37] Baranano DE, Rao M, Ferris CD, Snyder SH. Biliverdin reductase: a major physiologic cytoprotectant. Proc Natl Acad Sci U S A 2002;99(25):16093–16098. doi:10.1073/pnas.252626999, PMID:12456881.
[38] Stocker R, Glazer AN, Ames BN. Antioxidant activity of albumin-bound bilirubin. Proc Natl Acad Sci U S A 1987;84(16):5918–5922. doi:10.1073/pnas.84.16.5918, PMID:3475708.
[39] Heidari Nejad S, Azzam O, Schlaich MP. Dual Endothelin Antagonism with Aprocitentan as a Novel Therapeutic Approach for Resistant Hypertension. Curr Hypertens Rep 2023;25(10):343–352. doi:10.1007/s11906-023-01259-z, PMID:37566184.
[40] Schiffrin EL, Pollock DM. Endothelin System in Hypertension and Chronic Kidney Disease. Hypertension 2024;81(4):691–701. doi:10.1161/HYPERTENSIONAHA.123.21716, PMID:38059359.
[41] Liang HF, Yang X, Li HL, Li X, Tian JN, Su HG, *et al*. Activation of pregnane X receptor protects against cholestatic liver injury by inhibiting hepatocyte pyroptosis. Acta Pharmacol Sin 2025;46(1):147–158. doi:10.1038/s41401-024-01357-x, PMID:39112769.
[42] Russell TM, Richardson DR. The good Samaritan glutathione-S-transferase P1: An evolving relationship in nitric oxide metabolism mediated by the direct interactions between multiple effector molecules. Redox Biol 2023;59:102568. doi:10.1016/j.redox.2022.102568, PMID:36563536.
[43] Pecchiari M, Pontikis K, Alevrakis E, Vasileiadis I, Kompoti M, Koutsoukou A. Cardiovascular Responses During Sepsis. Compr Physiol 2021;11(2):1605–1652. doi:10.1002/cphy.c190044, PMID:33792902.
[44] Guo Q, Jin Y, Chen X, Ye X, Shen X, Lin M, *et al*. NF-κB in biology and targeted therapy: new insights and translational implications. Signal Transduct Target Ther 2024;9(1):53. doi:10.1038/s41392-024-01757-9, PMID:38433280.
[45] Prado AF, Batista RIM, Tanus-Santos JE, Gerlach RF. Matrix Metalloproteinases and Arterial Hypertension: Role of Oxidative Stress and Nitric Oxide in Vascular Functional and Structural Alterations. Biomolecules 2021;11(4):585. doi:10.3390/biom11040585, PMID:33923477.
[46] Rodríguez-Sánchez E, Navarro-García JA, Aceves-Ripoll J, González-Lafuente L, Baldan-Martin M, de la Cuesta F, *et al*. Prediction of the early response to spironolactone in resistant hypertension by the combination of matrix metalloproteinase-9 activity and arterial stiffness parameters. Eur Heart J Cardiovasc Pharmacother 2022;8(1):68–76. doi:10.1093/ehjcvp/pvaa086, PMID:32663251.
[47] Rushbrook SM, Kendall TJ, Zen Y, Albazaz R, Manoharan P, Pereira SP, *et al*. British society of gastroenterology guidelines for the diagnosis and management of cholangiocarcinoma. Gut 2024;73(1):16–46. doi:10.1136/gutjnl-2023-330029, PMID:37770126.
[48] Armstrong A, Pugh D, Basu N, Dhaun N. Current and future treatments for takayasu arteritis: toward cardiovascular risk modification. Circulation 2026;153(4):266–81. doi:10.1161/CIRCULATIONAHA.125.076308, PMID:41587271.
[49] Lajoye Q, Orieux A, Boyer A, Prevel R, Jozwiak M. Vasopressin and its analogues in patients with septic shock: holy grail or unfulfilled promise? Crit Care 2025;29(1):333–53. doi:10.1186/s13054-025-05540-2, PMID:40731360.